Finite Boundaries in Theories of Gravity

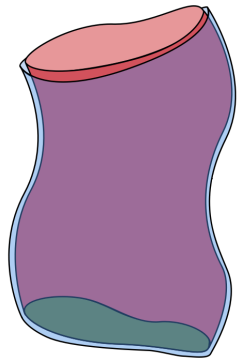

Dionysios Anninos

King's College London

Strings, Abu Dhabi, 9/1/2025

based on work with: Raúl Arias, Chiara Baracco, Damián Galante, Chawakorn Maneerat, Beatrix Mühlmann

1109.4942, 1110.3792 + 2206.14146, 2310.08648, 2402.04305, 2412.16305

The Royal Society

UKRI Science and Technology Facilities Council

KU Leuven

General Context

We are accustomed to gravitational theories with asymptotic boundaries at spatial/null infinity. One virtue is the provision of good gravitational observables.

In certain circumstances, we do not have this luxury. Examples include spacetimes containing cosmological horizons or compact Cauchy surfaces.

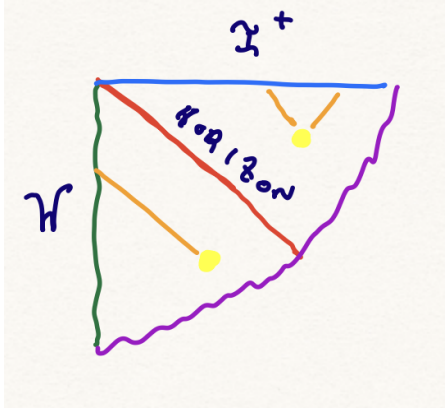

In those circumstances, we may have to confront a more quasilocal description.

Geheniau,Debever-Bergmann-Komar-...-York-...

Modern Context

It is also desirable to understand AdS/CFT at finite boundary.

...-de Boer,Verlinde,Verlinde-...-Heemskerk,Polchinski-...-Andrade,Kelly,Marolf,Santos-...

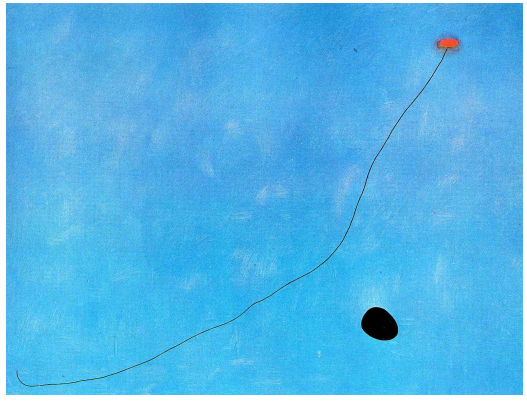

Moreover, a quasilocal description of the static patch, decorated with a timelike feature, may illuminate questions about the de Sitter event horizon.

...-D.A.,Hartnoll,Hofman-Coleman,Silverstein,Mazenc,Torroba-Banihashemi,Jacobson-Chandrasekaran,Longo,Penington,Witten-Loganayagam,Shetye-...

In this talk we will discuss four-dimensional general relativity in the presence of a finite size boundary in both Euclidean and Lorentzian signature, for general Λ.

The work is open-ended and ongoing. Here, we offer a status report.

Gravitational Worldtubes

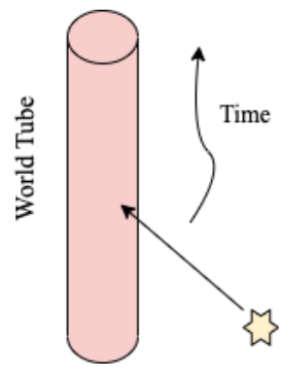

Dirichlet Initial Boundary Value Problem

A natural boundary condition is the Dirichlet one, whereby we fix the induced metric, g_{mn}, along the timelike boundary Γ, and Cauchy data along Σ.

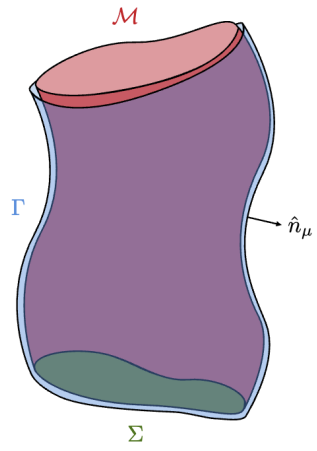

For generic g_{mn}, the Dirichlet problem may suffer existence/uniqueness issues. Near the Minkowski/Rindler corner one finds infinite solutions that are not fixed by initial data. Generic choices of boundary data at Γ can fail to yield a solution.

...-An,Anderson-...-D.A.,Galante,Maneerat-...

Euclidean Dirichlet Problem

In Euclidean signature one does not generically have an elliptic problem. This can affect the perturbative treatment of Euclidean path integrals.

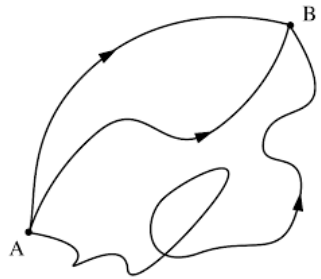

Also, for generic boundary data at Γ, there are existence issues, e.g. near a flat boundary $\delta_{h_{ij}}\mathcal{R} = 0$.

Avramidi,Esposito-...-Anderson-...-Witten-...

Nonetheless, specific Dirichlet boundary conditions display good properties.

Conformal Boundary Conditions

An and Anderson ('21) **propose**, instead, to fix the conformal class $[g_{mn}(x^m)]$ along with the trace of the extrinsic curvature, $K(x^m)$, on Γ.

York-...-Bredberg,Strominger-D.A.,Anous,Bredberg,Ng-Adam,Kitchen,Wiseman-...

In addition to data on Γ, we must impose appropriate Cauchy data along a spatial slice Σ that intersects Γ at $\partial\Sigma$. Moreover, additional initial data

$$\mathcal{C}_{\partial\Sigma} = \{\boldsymbol{\omega}(x^m), \dot{\boldsymbol{\omega}}(x^m)\}|_{\partial\Sigma}$$

is necessary to ensure uniqueness.

...-D.A.,Galante,Maneerat-Liu,Santos,Wiseman-...

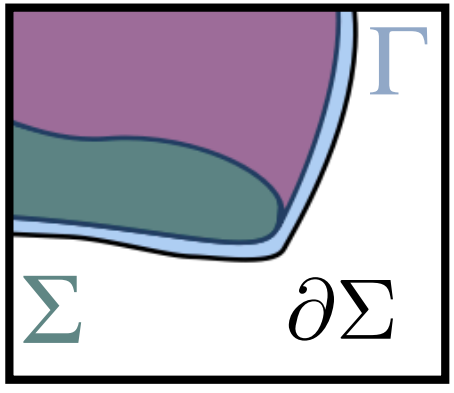

Conformal Brown-York Tensor

For conformal boundary data $[g_{mn}]$ and K:

$$T_{mn} = -\frac{e^{\omega}}{8\pi G_N}\left(K_{mn} - \frac{1}{3}Kg_{mn}\right) .$$

Note $T_m{}^m = 0$, and conserved for boundary conformal Killing vector fields.

York-...-An,Anderson-Odak,Speziale

T_{mn} receives contributions from the boundary data. The conserved quantities agree with those computed via Euclidean methods.

Hayward-...-Hawking,Hunter-Lehner,Myers,Poisson,Sorkin-...

Euclidean Conformal Boundary Conditions

Anderson ('08) established that CBCs are well-posed in Euclidean gravity. As a simple application, consider the 4d $\Lambda = 0$ Euclidean path integral with $S^2 \times S^1_\beta$ boundary, and constant K.

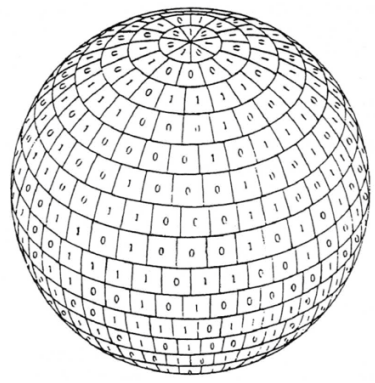

There are two branches of black hole saddles, one with positive specific heat. The Bekenstein-Hawking relation, at large temperature, reads

$$S_{\text{BH}} \approx \frac{4\pi^3}{G_N K^2}\left(\frac{1}{\beta^2} + \ldots\right)$$

D.A.,Galante,Maneerat-Banihashemi,Shaghoulian,Shashi

Linearised Dynamics for $S^2 \times \mathbb{R}$ with constant K

Spherically Symmetric Sector

Let us fix conformal boundary data

$$g_{mn}dx^m dx^n = e^{2\omega(x^m)}\left(-dt^2 + d\Omega^2\right) \ , \quad K = \text{const}$$

and fill Γ with a maximally symmetric bulk solution.

A spherically symmetric boundary mode, $\omega_0(t)$, exists for all Λ. Although locally a diffeomorphism, ω_0 carries non-vanishing energy. It obeys

$$\ddot{\omega}_0 = -\left(2 - \Lambda e^{2\omega_0}\right) - 2\dot{\omega}_0^2 + K e^{\omega_0}\sqrt{1 - \tfrac{\Lambda}{3}e^{2\omega_0} + \dot{\omega}_0^2} \ .$$

We must further fix the initial data $\{\omega_0, \dot{\omega}_0\}|_{\partial\Sigma}$ to ensure a unique evolution.

D.A.,Galante,Maneerat-Liu,Santos,Wiseman

Minkowski$_4$ Dynamics

We can decompose the modes in terms of the $SO(3)$ angular momenta (L, m). One collection of normal modes has regularly spaced real frequencies.

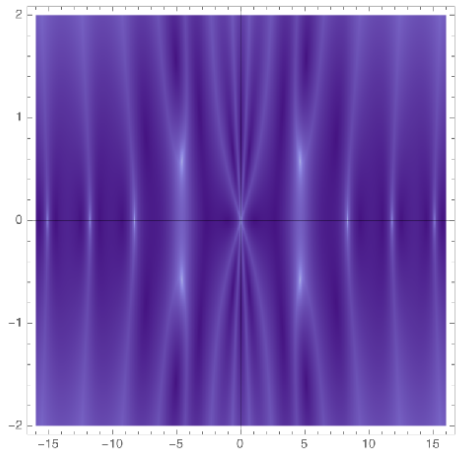

In addition, we uncover a quartet of complex frequencies for each $(L \geq 2, m)$,

$$\omega_L \approx \frac{K}{2}\left(\pm L \pm 0.34 i L^{1/3}\right) \ , \qquad L \gg 1 \ .$$

This suggests the vacuum is no longer the Minkowski filling.

DS_4 Cosmic Patch Dynamics

For $\Lambda = +\frac{3}{\ell^2}$, we find a deformation of the static patch quasinormal modes, as well as a set of complex frequencies modes whose structure depends on $K\ell$.

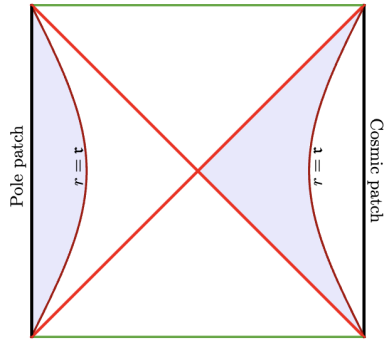

As $K\ell \to \infty$ (stretched horizon limit), the modes metamorphose to

$$\begin{aligned} \omega_L \ell &= \pm \frac{1}{\sqrt{2} K\ell} \sqrt{L(L+1)} - \frac{i}{4K^2\ell^2} \left(L(L+1) - 2\right) + \ldots \\ \omega_L \ell &= -\frac{i}{2K^2\ell^2} (L(L+1) - 2) + \ldots \end{aligned}$$

These are reminiscent of 'fluid-gravity' modes. Their bulk viscosity vanishes, in contrast to the classic work of Damour, Znajek, and Price & Thorne.

...-D.A.,Anous,Bredberg,Ng-...-D.A.,Galante,Maneerat

De Sitter Thermodynamics

dS_D horizon exhibits +ve specific heat for CBCs, contrasting the Dirichlet case.

Example: dS_3 Gibbons-Hawking entropy takes the form

$$\boxed{\mathcal{S}_{\rm dS} = 2\pi\sqrt{\frac{\mathfrak{c}}{3}\left(E(\beta) - \frac{\mathfrak{c}}{12}\right)} = \frac{2\pi^2\mathfrak{c}}{3\beta}}$$

where $\mathfrak{c} \equiv \frac{3\ell}{4G_N}\left(\sqrt{K^2\ell^2+4} - K\ell\right)$ is monotonic in $K\ell$.

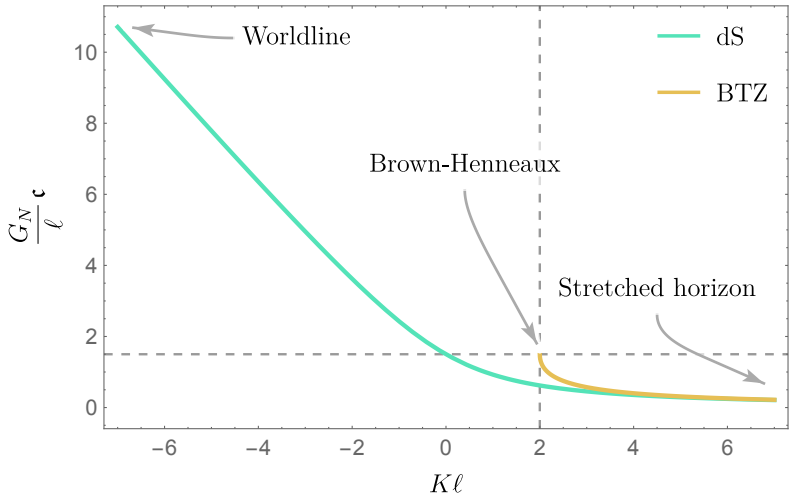

Aside: Boundary in 2D Quantum Gravity

Two-dimensional quantum gravity with $\Lambda > 0$ coupled to a $c \gg 1$ CFT contains a semiclassical dS_2 saddle.

The static patch on with a Dirichlet S^1 boundary of size β has

$$\mathcal{Z}_{\text{disk}}(\beta) = J_{-c}\left(\beta\sqrt{\Lambda}\right)$$

Though not positive definite, it exhibits critical points along β.

D.A.,Baracco,Mühlmann

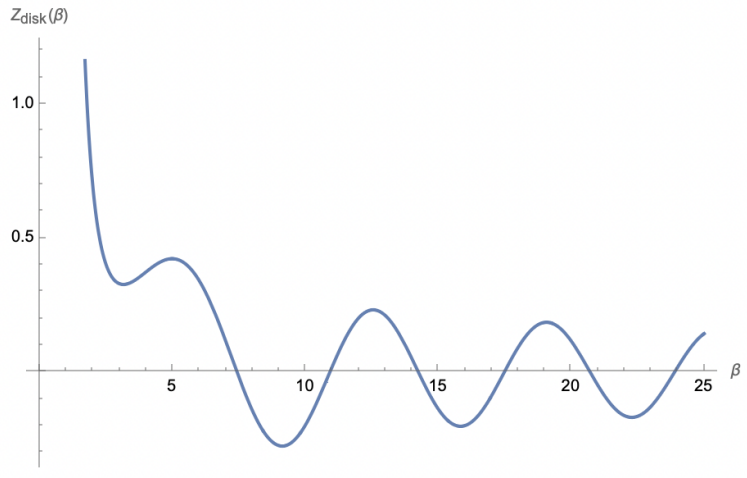

Near AdS_4/CFT_3

Asymptotically AdS_4

The boundary data of asymptotically AdS_4, with $\Lambda = -\frac{3}{\ell^2}$, consist of a conformal metric, $g^{(0)}_{mn}$, along with a conserved, traceless tensor $g^{(3)}_{mn}$.

$$\boxed{\frac{ds^2}{\ell^2} = d\rho^2 + e^{2\rho}\left(g^{(0)}_{mn} + e^{-2\rho}g^{(2)}_{mn} + e^{-3\rho}g^{(3)}_{mn} + ...\right)dx^m dx^n}$$

At the asymptotic boundary, $K = \frac{3}{\ell}$ for all Fefferman-Graham configurations. Thus, AdS_4/CFT_3 appears well-adapted to conformal boundary conditions.

Global AdS_4 Dynamics

By tuning away from $K = \frac{3}{\ell}$, we can move the asymptotic AdS_4 boundary. In addition to the collection of global AdS_4 normal modes, an additional set is uncovered, whose dispersion relation near $K = \frac{3}{\ell}$ goes as

$$\omega_L \ell = \pm\sqrt{L(L+1)-1} + \mathcal{O}(K\ell - 3) \ .$$

The complex modes of Minkowski space are retrieved at large $K\ell$.

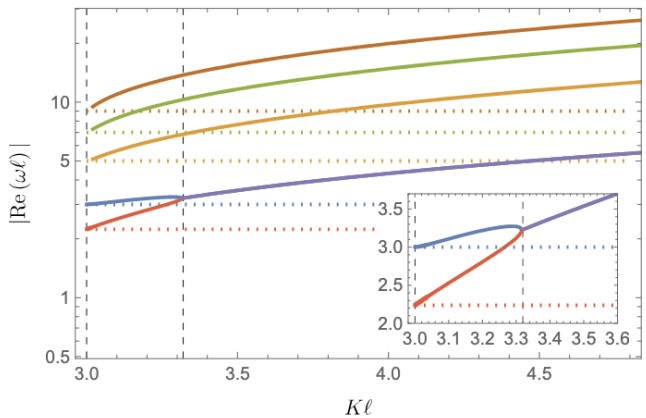

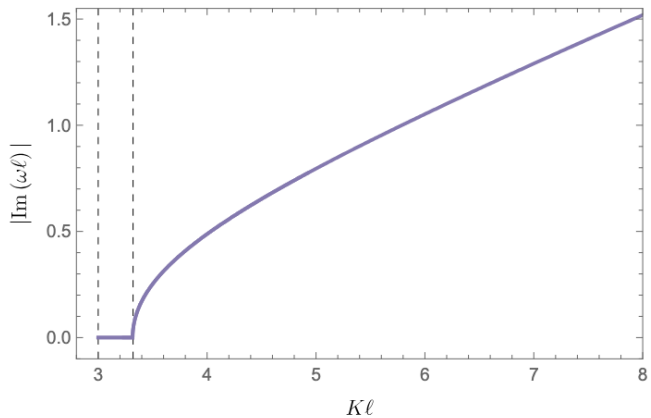

D.A.,Arias,Galante,Maneerat

Remark on New Modes

Degrees of freedom. The new modes are labeled by (L, m), with no bulk radial quantum number. They perturb the boundary Weyl factor. As $K \to \frac{3}{\ell}$ they parameterise a residual diffeomorphism preserving the Fefferman-Graham gauge.

Planar AdS$_4$. A linear analysis reveals similar modes. They can be expressed (locally) as diffeomorphisms and never exhibit complex frequencies.

Conformal Brown-York Tensor

Near the AdS_4 boundary

$$\boxed{T_{mn} = \frac{1}{8\pi G_N \ell} \frac{\mathcal{F}_{mn}[g^{(0)}_{mn}]}{\sqrt{K\ell - 3}} + \frac{3}{16\pi G_N \ell} g^{(3)}_{mn} + \ldots}$$

The leading term diverges as $K \to \frac{3}{\ell}$, and is ordinarily discarded as an immaterial divergence in AdS/CFT.

...-Balasubramanian,Kraus-de Haro,Skenderis,Solodukhin-...

At finite $K - \frac{3}{\ell}$, however, the additional term contributes in a finite way.

AdS$_4$ Black Hole

The high temperature limit of an AdS$_4$ black hole takes the following form

$$\boxed{S_{\text{BH}} = \frac{16\pi^3\ell^2}{81\,G_N}\left(K\ell - \sqrt{K^2\ell^2 - 9}\right)^2 \frac{1}{\beta^2} + \ldots}$$

The K dependent pre-factor is monotonic and tends to the Minkowski expression at large $K\ell$. As $K \to \frac{3}{\ell}$ it approaches the AdS$_4$/CFT$_3$ value.

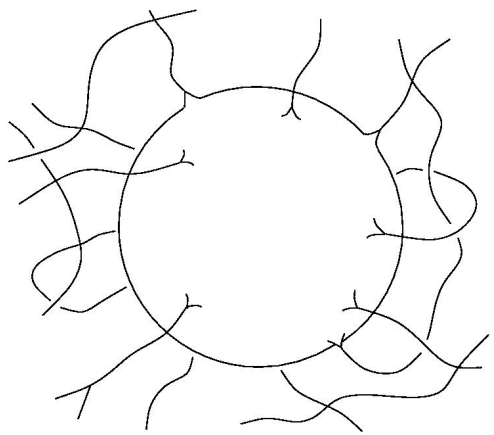

The boundary mode ω_0 'dresses' the black hole/brane and alters its energy.

Outlook

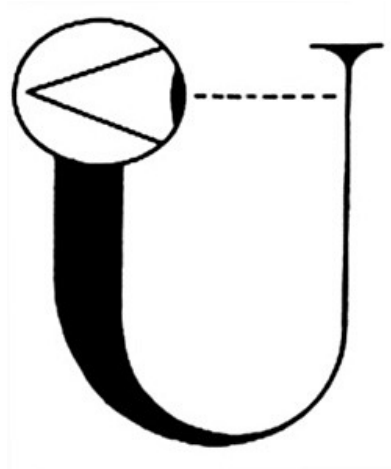

Imperfect Thoughts

The AdS_4/CFT_3 interpretation of CBCs was not answered. It seems tied to the ultraviolet structure of the dual CFT_3.

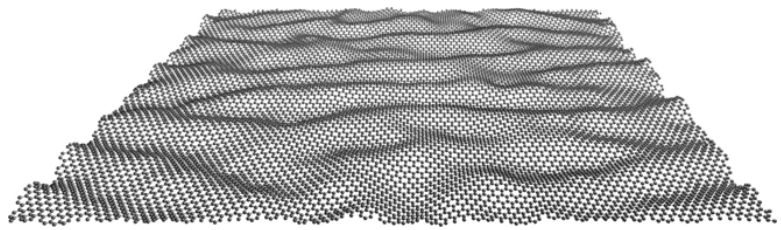

The appearance of a massless dispersion relation, and the presence of the dimensionful $K(x^m)$, evoke notions of conformal symmetry breaking.

Further Imperfect Thoughts

A concrete quantum object of interest is

$$\boxed{\mathcal{Z}[[g_{mn}], K(x^m)] = \int \mathcal{D}g_{\mu\nu} e^{-S_E[g_{\mu\nu}]}}$$

Nothing precludes us from computing this object for $\Lambda \in \mathbb{C}$.

$\mathcal{Z}$ resembles a Legendre transform w.r.t. the AdS Dirichlet boundary volume form. This cannot be precise; the Dirichlet problem is not generically well-posed.

Future Applications

CBCs appear to play an interesting role for a variety of timelike surfaces: dS/black hole (stretched) horizons, thickened worldlines, and near-AdS boundaries.

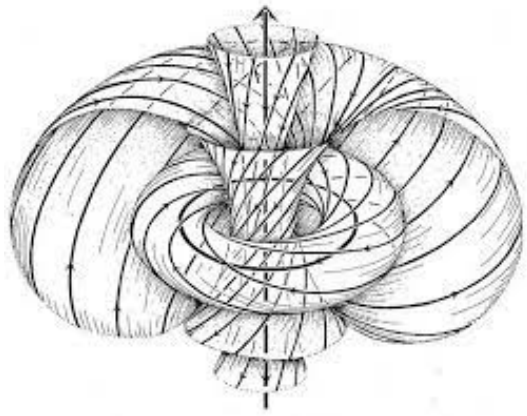

They may illuminate how to split/join Euclidean path integrals, and in turn dispel puzzles on the physical properties of the Euclidean dS_D (sphere) path integral. For example, at the saddle point level, and for $\Lambda > 0$

$$\mathcal{Z}^{\text{pole}}[-K, S^2 \times S^1_*] \times \mathcal{Z}^{\text{cosmic}}[+K, S^2 \times S^1_*] = e^{\mathcal{S}} \approx \mathcal{Z}[S^4]$$

Thank you for your time!

Extra Slide I: Sphere Partition Function

To one-loop,

$$\boxed{\mathcal{Z}[S^4] = e^{\mathcal{S}} \times i^{1+5}\mathcal{S}^{-\frac{10}{2}} \exp \int_{\mathbb{R}^+} \frac{d\mathrm{t}}{2\mathrm{t}} \left(\chi_{\mathsf{bulk}}(\mathrm{t}) - \chi_{\mathsf{edge}}(\mathrm{t})\right) \ .}$$

...-D.A.,Denef,Law,Sun-...

The $\chi(\mathrm{t})$ are Harish-Chandra characters of the $SO(1,4)$ spin-2 discrete series irrep.

$$\chi_{\mathsf{bulk}}(\mathrm{t}) = \frac{10q^3 - 6q^4}{(1-q)^3} \ , \qquad \chi_{\mathsf{edge}}(\mathrm{t}) = \frac{10q^2 - 2q^3}{1-q} \ .$$

Extra Slide II: DS_4 Phase Diagram

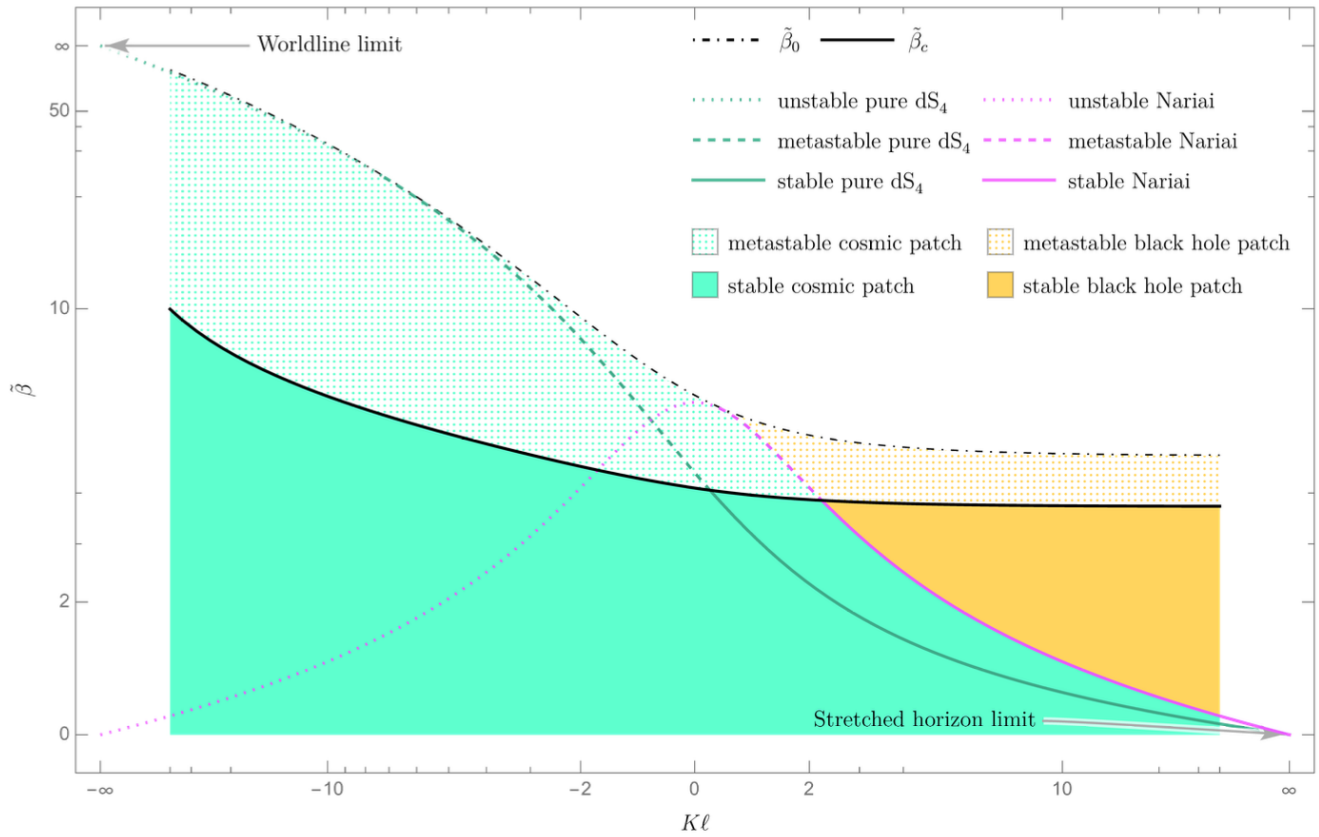

Fig. 10: Phase diagram of conformal dS_4 thermodynamics for static and spherically symmetric configurations. The number of different solutions co-existing at a given point in the phase diagram depends on whether the point lies above or below the $\tilde{\beta}_0$ curve (dot-dashed black curve). Above that curve, only one pole patch solution exists. Below the $\tilde{\beta}_0$ curve, apart from a pole patch solution, there co-exist two additional cosmic/black hole patches, one with negative and one with positive C_K. The curve of critical inverse conformal temperature $\tilde{\beta}_c$ is shown in thick black, above which the pole patch is thermodynamically preferred. In the region bounded by $\tilde{\beta}_0$ and $\tilde{\beta}_c$ curves, shaded in green (yellow) halftone, the cosmic (black hole) patch is metastable. For $\tilde{\beta}_c > \tilde{\beta}$, the cosmic (black hole) patch is stable with the associated region shaded in solid green (yellow). The dark green and purple curves represent pure dS_4 and Nariai patches. Both curves are divided into three segments: stable, metastable, and unstable, which are shown as thick, dashed and dotted curves, respectively. The (meta)stable Nariai curve marks the separation of the (meta)stable cosmic patch and black hole patch regions.

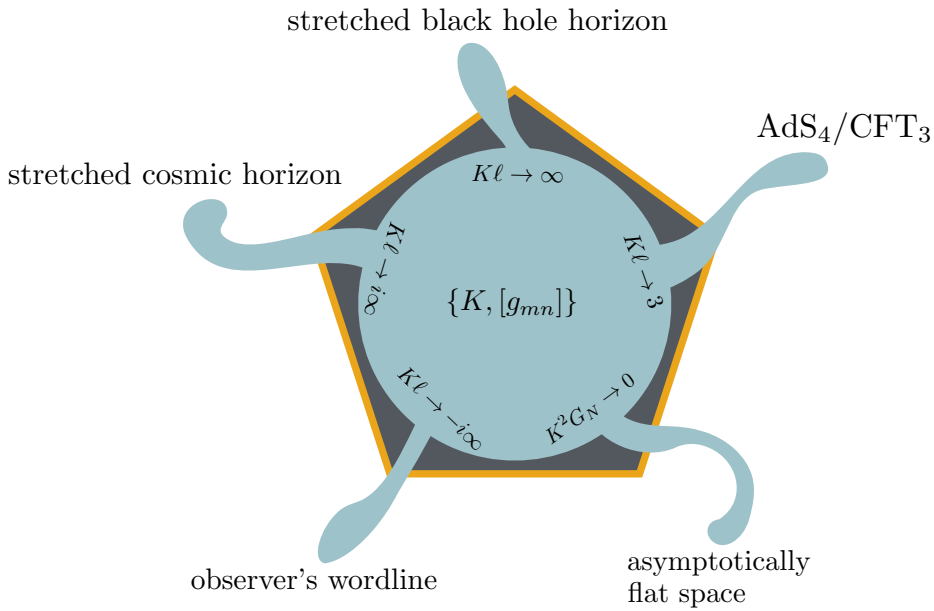

Image courtesy of Damián Galante